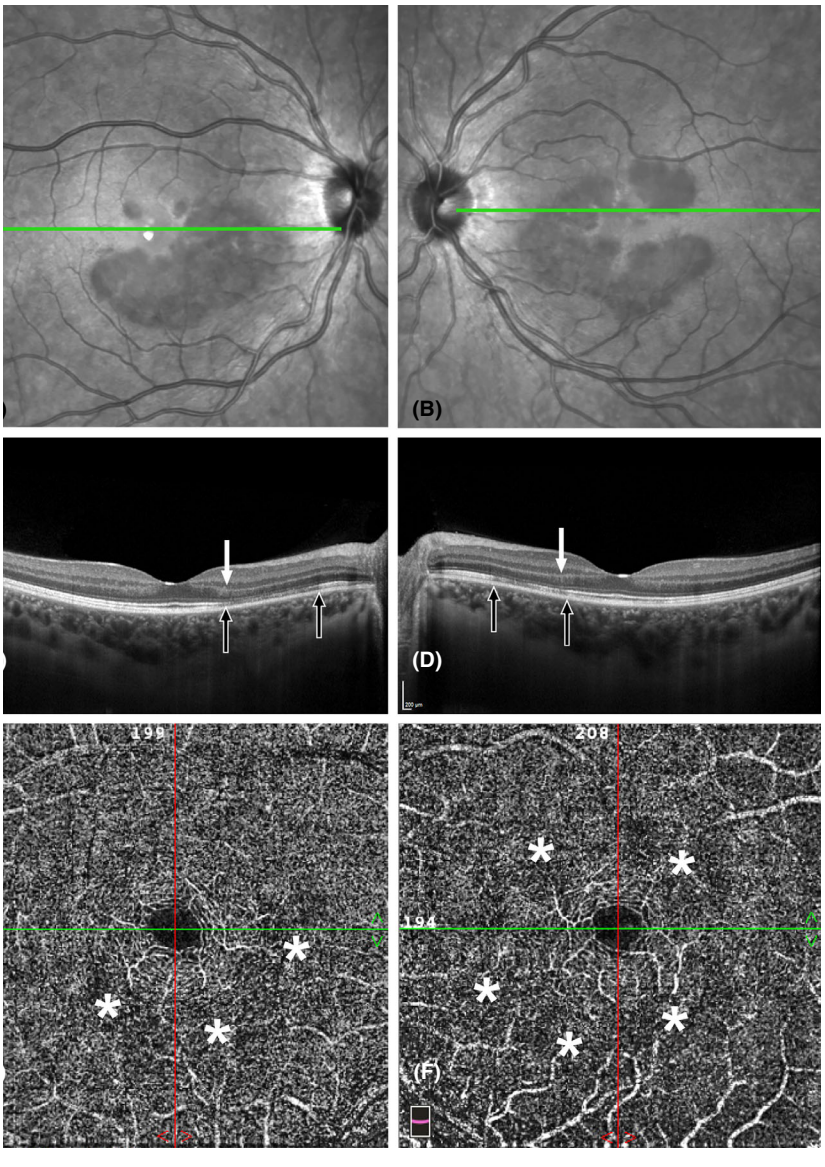

Fig. 1. (A,B) Near-infrared imaging of right eye (A) and left eye (B) shows multiple hyporeflective lesions in the paracentral macula in both eyes. The small lesions have a petaloid shape, but the majority of lesions are large and confluent, almost forming a ring around the fovea. (C, D) Spectral-domain optical coherence tomography of right eye (C) and left eye (D) at the level of the green line in Figure A, B, shows interruption of the ellipsoid zone and the interdigitation zone (black arrows). There are also hyperreflective changes (white arrow) within the outer nuclear layers. (E, F) Optical coherence tomography angiography of the right eye (E) and left eye (F) shows multiple areas of decreased vascular flow signal (asterisks) at the level of the deep capillary plexus corresponding to the lesions visible in the near-infrared reflectance imaging.

The pathophysiology of AMN is a non-inflammatory vaso-occlusive disorder of retinal capillaries. Optical coherence tomography (OCT) and OCTA changes related to capillary vasculopathy have been reported in the DCP and/or choriocapillaris (Casalino et al. 2019), (Fawzi et al. 2012). The typical fundus abnormality of AMN is one or more wedge-shaped, well-delineated lesions pointing to the fovea (Bhavsar et al. 2016). AMN following COVID-19 infection is rare. Two previous published cases (Gascon et al. 2020; Virgo & Mohamed 2020) reported small, focal petaloid lesions in one affected eye. However, our patient demonstrated unusually large, confluent lesions in both eyes, which suggested a large area of retinal pathology. We wonder whether endotheliopathy due to direct SARS-CoV-2 infection predisposes to greater retinal ischaemia and larger lesions of AMN (Iba et al. 2020). Systematic ophthalmologic examination of patients with coronavirus disease may clarify the prevalence and clinical profile of AMN associated with COVID-19.

References

Bhavsar KV, Lin S, Rahimy E, Joseph A, Freund KB, Sarraf D & Cunningham ET (2016): Acute macular neuroretinopathy: a comprehensive review of the literature. Surv Ophthalmol **61**: 538–565.

Casalino G, Arrigo A, Romano F, Munk MR, Bandello F & Parodi MB (2019): Acute macular neuroretinopathy: pathogenetic insights from optical coherence tomography angiography. Br J Ophthalmol **103**: 410–414.

Fawzi AA, Pappuru RR, Sarraf D et al. (2012): Acute macular neuroretinopathy: long-term insights revealed by multimodal imaging. Retina **32**: 1500–1513.

Gascon P, Briantais A, Bertrand E et al. (2020): Covid-19-associated retinopathy: a case report. Ocul Immunol Inflamm **28**: 1293–1297.

Iba T, Connors JM & Levy JH (2020): The coagulopathy, endotheliopathy, and vasculitis of COVID-19. Inflamm Res **69**: 1181–1189.

Virgo J & Mohamed M (2020): Paracentral acute middle maculopathy and acute macular neuroretinopathy following SARS-CoV-2 infection. Eye **34**: 2352–2353.

Received on February 13th, 2021.
Accepted on May 1st, 2021.

Correspondence:
Aki Kawasaki
Avenue de France 15
Lausanne, Switzerland
Tel. +41 21 626 8660
Fax: +41 21 626 8666
Email: aki.kawasaki@fa2.ch

Spectral calibration of fluorescence lifetime imaging ophthalmoscopy

Rowena Schultz,[1] Matthias Klemm,[2] Daniel Meller[1] and Martin Hammer[1,3]

[1]Department of Ophthalmology, University Hospital Jena, Jena, Germany; [2]Institute of Biomedical Engineering and Informatics, Technical Univ. Ilmenau, Ilmenau, Germany; [3]Center for Medical Optics and Photonics, Univ. of Jena, Jena, Germany

doi: 10.1111/aos.14950

Editor,

Fundus autofluorescence (FAF) is a standard ophthalmic imaging modality. Quantitative FAF and fluorescence lifetime imaging ophthalmoscopy (FLIO) are attempts to measure FAF parameters. Primarily, FLIO gives fluorescence lifetimes. However, as measurements are taken in two spectral channels (500–560 nm and 560–720 nm) upon fluorescence excitation at 470 nm, it also yields spectral information. Formerly, we reported this information as the ratio of the measured intensity in the short and long wavelength channel (Hammer et al. 2020), denoted as the spectral ratio (sr). Here, we introduce a calibration of the sr to provide spectral information as the emission peak wavelength (EPW) in nanometer.

We performed FLIO measurements of FAF in 43 young healthy subjects (age: 23.8 ± 3.4 years). Measurements from the lens were taken in a cohort of 62 healthy subjects (age: 41.0 ± 18.6 years) with no cataract by focussing the FLIO scanner to the anterior part of the eye. We found the mean sr to be 0.991 ± 0.141 for the lens and 0.446 ± 0.057 for the FAF, measured in the outer ring of the standard ETDRS grid. We related these values to emission spectrum peaks of lens and fundus fluorescence found in the literature. Zuclich et al. (2005) reported a lens emission peak at 515 nm (average subject age: 44.5 ± 16.9 years) what is in agreement with Delori (1994) and Kurzel et al. (1973). The FAF peak emission wavelength is reported as 621 ± 6 nm upon 470 nm excitation 7° temporal to the fovea in healthy subjects (Delori et al. 1995). From these data and our measured sr, we established the following linear relationship: EPW[nm] = −195*sr + 708. This can be used to derive the approximate peak wavelength of FAF and to generate EPW images. An example is given in Fig. 1, left. This gives a colour-coded representation (see scale bar) of the EPW. This is lowest in the optic disc, but also shorter emission wavelength was found in the fovea than extrafoveally. In our cohort of 43 young, healthy subjects, we found highly significant differences in EPW for the centre, the inner and the outer ring of the ETDRS grid (Fig. 1, right) by a general linear model for repeated measures and Bonferroni correction for repeated testing (SPSS 27). This finding of an emission peak at shorter wavelength in the fovea than in the periphery is in agreement with (Delori et al. 1995) and might indicate a foveal lipofuscin composition, different from the para-foveal one, but also may be influenced by the macular pigment or by a higher foveal melanin concentration.

In conclusion, the described spectral calibration enables the measurement of EPW for each pixel of the FLIO image. In subsequent studies, this can relate the investigation of spectral differences within images as well as between patient groups to published spectral characteristics of fluorophores and tissues.

References

Delori FC (1994): Spectrometer for noninvasive measurement of intrinsic fluorescence and reflectance of ocular fundus. Appl Optics **33**: 7439–7452.

Delori FC, Dorey KC, Staurenghi G, Arend O, Goger DC & Weiter JJ (1995): In vivo fluorescence of the ocular fundus exhibits retinal pigment epithelium lipofuscin characteristics. Invest Ophthalmol **36**: 718–729.

Hammer M, Schultz R, Hasan S et al. (2020): Fundus autofluorescence lifetimes and spectral features of soft drusen and hyperpigmentation in age-related macular degeneration. Transl Vis Sci Technol **9**: 20.

Kurzel RB, Wolbarsht ML & Yamanashi BS (1973): Spectral studies on normal and cataractous intact human lenses. Exp Eye Res **17**: 65–71.

Zuclich JA, Previc FH, Novar BJ & Edsall PR (2005): Near-UV/blue light-induced fluorescence in the human lens: potential interference with visual function. J Biomed Opt **10**: 44021.

Received on May 10th, 2021.
Accepted on May 31st, 2021.

Correspondence:
Martin Hammer, PhD
Department of Ophthalmology
University Hospital Jena
Am Klinikum 1
07747 Jena
Germany
Tel: +49-3641-9390860
Fax: +49-3641-9390867
Email: martin.hammer@med.uni-jena.de

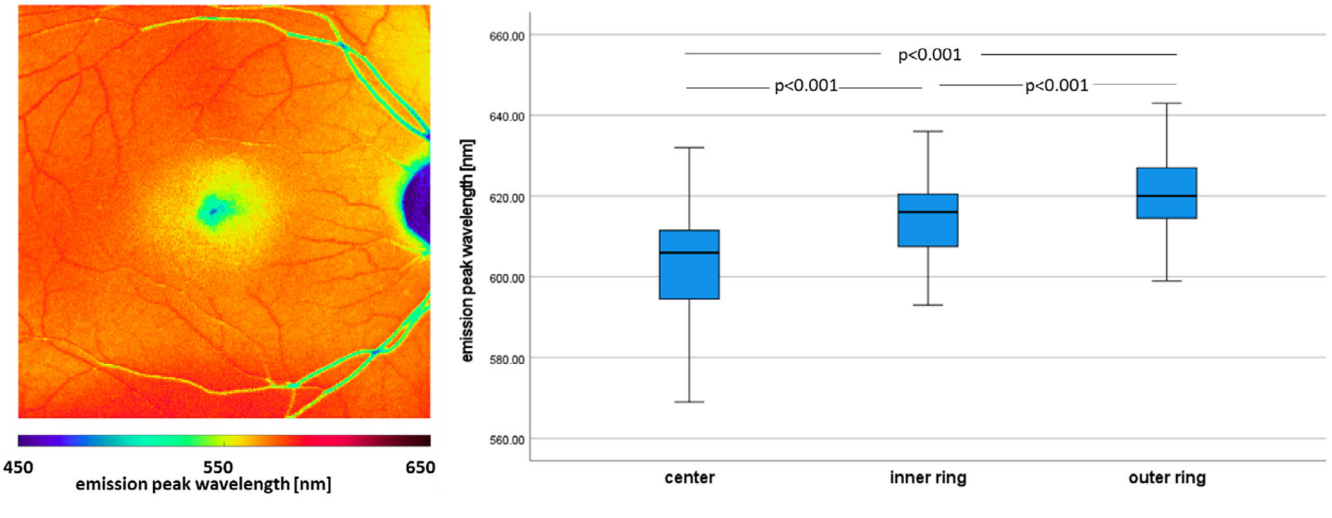

Fig. 1. Left: colour-coded image of the emission peak wavelength (EPW) for a 25-year-old healthy male subject. Right: boxplot of the EPW of 43 young healthy subjects, averaged over the centre, the inner and the outer ring of the standard ETDRS grid.